FEBS Letters 589 (2015) 3126–3132

journal homepage: www.FEBSLetters.org

COX assembly factor ccdc56 regulates mitochondrial morphology by affecting mitochondrial recruitment of Drp1

Reiko Ban-Ishihara [a,1], Shiho Tomohiro-Takamiya [b,1], Motohiro Tani [b], Jacques Baudier [c], Naotada Ishihara [a,*], Osamu Kuge [b,*]

[a] Department of Protein Biochemistry, Institute of Life Science, Kurume University, Kurume 839-0864, Japan
[b] Department of Chemistry, Faculty of Sciences, Kyushu University, Fukuoka 812-8581, Japan
[c] INSERM, Unité 873, Grenoble F-38054, France

ARTICLE INFO

Article history:
Received 1 June 2015
Revised 31 July 2015
Accepted 31 August 2015
Available online 7 September 2015

Edited by Barry Halliwell

Keywords:
Organelle
Mitochondria
Mitochondrial fission
Cytochrome oxidase (COX)
Drpl

ABSTRACT

Mitochondria are dynamic organelles that alter their morphology in response to cellular signaling and differentiation through balanced fusion and fission. In this study, we found that the mitochondrial inner membrane ATPase ATAD3A interacted with ccdc56/MITRAC12/COA3, a subunit of the cytochrome oxidase (COX)-assembly complex. Overproduction of ccdc56 in HeLa cells resulted in fragmented mitochondrial morphology, while mitochondria were highly elongated in ccdc56-repressed cells by the defective recruitment of the fission factor Drp1. We also found that mild and chronic inhibition of COX led to mitochondrial elongation, as seen in ccdc56-repressed cells. These results indicate that ccdc56 positively regulates mitochondrial fission via regulation of COX activity and the mitochondrial recruitment of Drp1, and thus, suggest a novel relationship between COX assembly and mitochondrial morphology.

1. Introduction

Mitochondria are double membrane-bound organelles with essential roles in diverse metabolic and signaling pathways [1], and have extremely different morphologies depending on cell type. Even in the same cell, such as mammalian fibroblasts, mitochondria can exhibit a range of morphologies, from small spheres or short rods to long tubules. The overall shape of mitochondria is regulated by fusion and fission, and several components of the core machinery for fusion (Mfn1, Mfn2, and OPA1) and fission (Drp1 and the mitochondrial receptors Mff, MiD49, and MiD51) have been identified in mammalian cells [2–5]. In the absence of fusion (for example, in Mfn1 and -2 double null mutant cells), ongoing fission events result in the formation of fragmented mitochondria, while a decrease of fission relative to fusion (for example, in cells expressing a dominant negative form of Drp1) results in elongated mitochondria. As well as controlling the shape of mitochondria, fusion and fission are crucial for maintaining their function, including respiratory capacity, and play key roles in mammalian development [6], several neurodegenerative diseases [6], and apoptosis [7]. Although several components of the core fusion and fission machinery have been identified, the detailed mechanisms and regulation of mitochondrial fusion and fission remain to be elucidated. In this study, we identified a mitochondrial membrane protein, coiled-coil domain-containing protein 56 (ccdc56), as a protein that regulates mitochondrial fission.

2. Materials and methods

2.1. Antibodies

The following commercial antibodies were used: mouse monoclonal anti-DNA (Progen); anti-Drp1 (BD Transduction);

Abbreviations: ccdc56, coiled-coil domain-containing protein 56; COX, cytochrome oxidase; Drp1, dynamin-related protein; FBS, fetal bovine serum; mtDNA, mitochondrial DNA; PDI, protein disulfide isomerase; siRNA, short-interfering RNA

Author contributions: R.B.-I. and S.T.-T. performed and analyzed experiments. M.T. and J.B. preliminary performed and analyzed experiments. N.I. and O.K. designed the experiments and wrote the paper.

* Corresponding authors.
E-mail addresses: ishihara_naotada@kurume-u.ac.jp (N. Ishihara), kuge@chem.kyushu-univ.jp (O. Kuge).

[1] These authors contributed equally to this work.

http://dx.doi.org/10.1016/j.febslet.2015.08.039
0014-5793/

anti-β-actin, anti-HA and anti-FLAG (Sigma); anti-MTCO1 (COX I), anti-MTCO2 (COX II), and MitoProfile Total OXPHOS Rodent WB Antibody Cocktail (Abcam); rabbit monoclonal anti-COX IV, anti-GAPDH, and rabbit polyclonal anti-Drp1 (pS637) (Cell Signaling); rabbit polyclonal anti-Tom20, -anti-HSP60, anti-HA, and a mouse monoclonal anti-actin and anti-myc (Santa Cruz); anti-protein disulfide isomerase (PDI) (Stressgen); anti-Mff (Proteintech). Rabbit polyclonal anti-Tom40 antibodies were a kind gift from Drs. Katsuyoshi Mihara (Kyushu University) and Toshihiko Oka (Kyushu University). Rabbit polyclonal antibodies against ATAD3 [8] were described. Horseradish peroxidase-conjugated secondary antibodies were purchased from BIOSOURCE or Molecular Probes. Alexa Fluor 488-, 568-, or 660-labeled goat anti-mouse IgG, IgM or anti-rabbit IgG were purchased from Molecular Probes.

2.2. Cell culture

HeLa cells and HeLa cells expressing mitochondria-targeted DsRed (mitRFP) [9] were cultured in ES medium (Nissui Pharmaceutical Co.) supplemented with 6% fetal bovine serum (FBS) (SIGMA), penicillin G (100 units/ml), and streptomycin sulfate (100 μg/ml), or in Dulbecco's modified Eagle's medium (Wako) supplemented with 10% FBC (Invitrogen) under a 5% CO_2 atmosphere at 37 °C.

2.3. Plasmid construction and transfection

To construct a HA-tagging plasmid, a DNA fragment encoding an HA epitope tag followed by a stop codon was amplified by PCR using primer-template oligonucleotides 5′-CCAGCA CAGTGGCGGCCGCTCGAGTACCCATACGACGTACCAGAT-3′ and 5′-T TCGAAGGGCCCTCTAGATCAAGCGTAATCTGGTACGTCGTATGGGTA-3′, digested with *NotI* and *Xbal*, and then inserted to the pcDNA3.1/myc-His A vector (Invitrogen) at the *NotI* and *XbaI* sites. The resulting vector was designated as pcDNA3.1/HA. To construct a plasmid encoding C-terminally HA tagged ccdc56, a cDNA fragment encoding ccdc56 was amplified from the pGADT7 plasmid carrying ORF of ccdc56 (Clontech) by PCR using a forward primer (ATTGAATTCGCCATGGCGTCTTCGGG) containing an *EcoRI* site and a reverse primer (ATTCTCGAGGGACCCTGACGCCCTTGCCA) containing an *XhoI* site. The PCR products were digested with *EcoRI* and *XhoI*, and then inserted in-frame into pcDNA3.1/HA using the corresponding restriction enzyme sites, which yielded pcDNA3.1-ccdc56-HA. Transfection of HeLa cells with pcDNA3.1-ccdc56-HA was performed using Lipofectamine 2000 (Invitrogen) according to the manufacturer's instructions.

2.4. Subcellular localization of ccdc56

HeLa cells transfected with an ccdc56-HA expression plasmid were washed with PBS, scraped off and then suspended in a homogenization buffer (10 mM HEPES-KOH (pH 7.4), 70 mM sucrose, and 0.22 M mannitol) containing a protease inhibitor cocktail (Complete EDTA-free (Roche Diagnostics)). The cell suspension was passed 30 times through a 27-gauge needle. After brief centrifugation (900×*g*, 5 min), the supernatant was centrifuged at 5000×*g* for 10 min. The resultant pellet was resuspended in the original volume of the homogenization buffer and saved as the mitochondrial fraction. The resultant supernatant was further centrifuged at 100 000 × *g* for 60 min to obtain microsomal and cytosolic fractions. The microsomal fraction pellet was resuspended in the original volume of the homogenization buffer and saved. Proteins in equal volumes of the total, mitochondrial, microsomal and cytosolic fractions were separated by SDS–PAGE, and Western blot detection was then performed with various antibodies.

2.5. Extraction of ccdc56 from mitochondria

The mitochondrial fraction was centrifuged at 5000×*g* for 10 min, and the pellet was resuspended in control buffer (40 mM Tris–HCl (pH 7.4), 150 mM NaCl), the same buffer containing 1% Triton X-100, or 0.1 M Na_2CO_3 buffer (pH 11.5). The suspension was incubated at 4 °C for 30 min and then centrifuged for 30 min at 100 000×*g*, and the resulting pellet was resuspended in the original volume of homogenization buffer. Proteins in equal volumes of the pellet and supernatant fractions were separated by SDS–PAGE, and Western blot detection was then performed with various antibodies.

2.6. RNA interference

Two short-interfering RNA (siRNA) duplexes targeting human ccdc56 (siGENOME: "siRNA-1" and "siRNA-3") as well as a non-targeting siRNA (siCONTROL Non-Targeting siRNA #2 D-001210-02) were purchased from Dharmacon. The target sequences of siRNAs "ccdc56-R1" and "ccdc56-R2" were 5′-GAAGCUGACACCCGAG CAA-3′ and 5′-GGUUACACCUUCUACUCGA-3′, respectively (Bonac).

To examine mitochondrial morphology, HeLa cells were transfected with control non-targeting siRNA duplex or ccdc56-targeting siRNA duplexes, using Lipofectamine 2000 or RNAiMAX (Invitrogen) according to the manufacturer's instructions. After two days, the cells were transfected again and cultured for a further two days. At two days or four days after the first transfection, the indirect immunofluorescence assay was carried out. Mock-transfected cells were prepared by the same procedure without siRNA duplexes.

To test the efficiency of ccdc56-depletion by siRNAs, 2×10^4 HeLa cells were seeded into the wells of a 24-well plate in Opti-MEM (Invitrogen) supplemented with 10% FBS, and after incubation for 24 h, the cells were cotransfected with plasmid pcDNA3.1-ccdc56-HA encoding ccdc56-HA (0.4 μg) and 10 pmol of a non-targeting siRNA duplex or a mixture of two ccdc56-targeting siRNA duplexes, using Lipofectamine 2000 (Invitrogen) according to the manufacturer's instructions. After two days incubation, the cells were lysed for immunoblot analysis. RT-PCR, immunoprecipitation, immunofluorescence analysis, SDS–PAGE and immunoblotting were analyzed as described previously [9,10].

3. Results and discussion

We identified human ccdc56, also known as MITRAC12 or COA3 [11–13], through a yeast two-hybrid system as a protein that interacts with the mitochondrial protein ATAD3 (also called AAA-TOB3), which has been suggested to play a role in tumor progression [14,15], and to be associated with mitochondrial DNA (mtDNA) nucleoids [16–18]. We confirmed their physical interaction in HeLa cells by co-immunoprecipitation experiments after crosslinking (Fig. 1A). Full-length cDNA clones of human ccdc56 were found previously on large-scale cDNA sequencing [19,20], and its sequence predicts a protein of 106 amino acid residues, which is conserved in chimpanzee, dog, cow, mouse, rat, chicken, and zebrafish (Fig. 1B). Ccdc56 was reported as a mitochondrial membrane protein [11–13], and we confirmed that ccdc56-HA transiently expressed in HeLa cells was localized in the mitochondria, as described below. Immunofluorescence microscopic analysis showed that ccdc56-HA colocalized with mitochondrial RFP or ATAD3A (Fig. 1E). When a post-nuclear supernatant of HeLa cells producing ccdc56-HA was fractionated into mitochondrial, microsomal, and cytosolic fractions, ccdc56-HA was recovered in the mitochondrial fraction containing the mitochondrial marker protein Tom40 (Fig. 1C). In contrast, ccdc56-HA was undetectable in

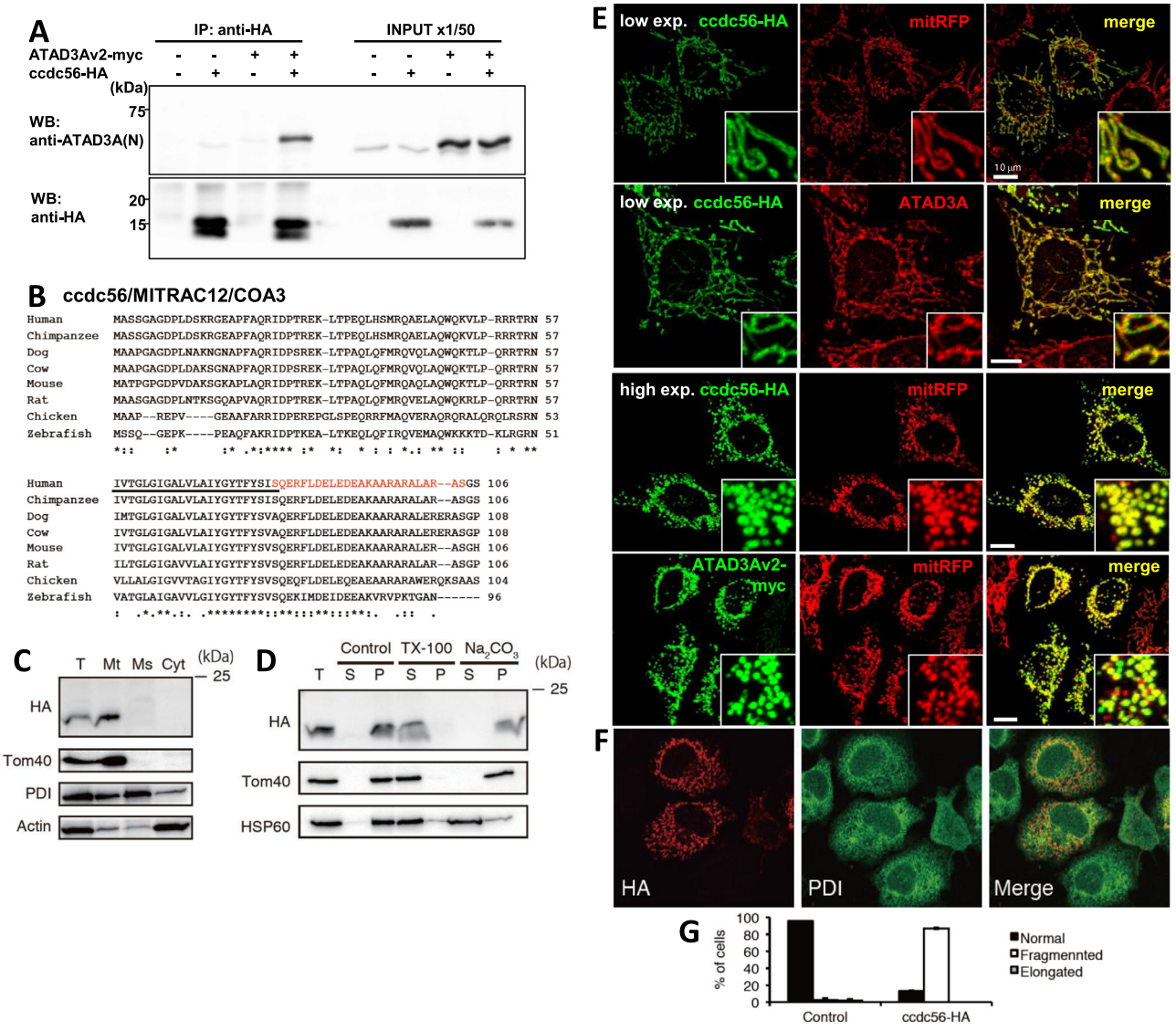

Fig. 1. Ccdc56 interacts with ATAD3A in mitochondria and affects mitochondrial morphology. (A) HeLa cells were transfected with human ccdc56-HA and ATAD3A variant 2-myc. The cells were treated with 1% formaldehyde for 10 min, immunoprecipitated with an anti-HA antibody, then analyzed by immunoblotting with the indicated antibodies. (B) Multiple sequence alignment of the predicted amino acid sequences of the ccdc56 proteins of human (NP_001035521.1*), chimpanzee (XP_001160561.1*), dog (XP_537635.1*), cow (NP_001029855.1*), mouse (NP_080894.1*), rat (XP_573196.1*), chicken (XP_001234221.1*), and zebrafish (NP_001108388.1*), performed with the ClustalW2 program, is shown. A transmembrane segment predicted with the TMHMM algorithm is underlined. Amino acid residues forming a coiled-coil domain are shown in red letters. *NCBI reference sequences. (C) Total lysate (T) from HeLa cells producing ccdc56-HA was fractionated into mitochondrial (Mt), microsomal (Ms), and cytosolic (Cyt) fractions. These fractions were subjected to immunoblotting analysis using antibodies against the HA epitope, mitochondrial outer-membrane protein Tom40, ER protein PDI, and cytosolic protein actin. (D) The mitochondrial fraction prepared from HeLa cells producing ccdc56-HA was suspended in a buffer (40 mM Tris–HCl pH 7.4, 150 mM NaCl) (Control), the same buffer containing 1.0% Triton X-100 (TX-100), or 0.1 M Na_2CO_3 buffer (pH 11.5) (Na_2CO_3), centrifuged to obtain the supernatant (S) and pellet (P) fractions, and then analyzed by immunoblotting with antibodies against the HA epitope, integral membrane protein Tom40, and mitochondrial matrix protein HSP60. (E) HeLa cells stably expressing mitochondrial RFP or normal HeLa cells were transfected with the indicated expression plasmids. These cells were fixed, permeabilized, and then immunostained with antibodies against HA, myc or ATAD3A. Images were acquired by confocal microscopy. Enlargements are presented to show structural details. (F) HeLa cells transfected with the ccdc56-HA expression plasmid were subjected to indirect immunofluorescence analysis with a monoclonal anti-HA antibody and polyclonal anti-PDI antibodies, and then analyzed by confocal microscopy. (G) Percentages of cells having normal, fragmented, elongated, or aggregated mitochondria among untransfected cells (Control) and cells overproducing ccdc56-HA. The data represent the mean ± standard deviation (S.D.) of three independent experiments (100 cells scored per experiment).

the microsomal and cytosolic fractions, which contained the endoplasmic reticulum (ER) marker protein PDI and the cytosolic marker protein actin (Fig. 1C). According to the SOSUI and TMHMM algorithms, ccdc56 is predicted to have a single transmembrane segment. To determine whether ccdc56 is an integral membrane protein, mitochondria of HeLa cells producing ccdc56-HA were subjected to alkaline (0.1 M Na_2CO_3) and detergent (1% Triton X-100) treatment, followed by ultracentrifugation. Upon alkaline treatment, the majority of ccdc56-HA was found in the membrane pellet fraction (Fig. 1D). In addition, the majority of ccdc56-HA was released into the supernatant upon detergent treatment followed by ultracentrifugation. This behavior of ccdc56-HA resembled that of the integral membrane protein Tom40, but was different from that of the matrix protein HSP60 (Fig. 1D). These results confirmed that ccdc56 is a mitochondrial membrane protein, consistent with the data showing this protein interacts with the inner membrane protein ATAD3 (Fig. 1A) and previous reports showing that ccdc56 is a subunit of the assembly factor of cytochrome c oxidase (COX) in the mitochondrial inner membrane [11–13].

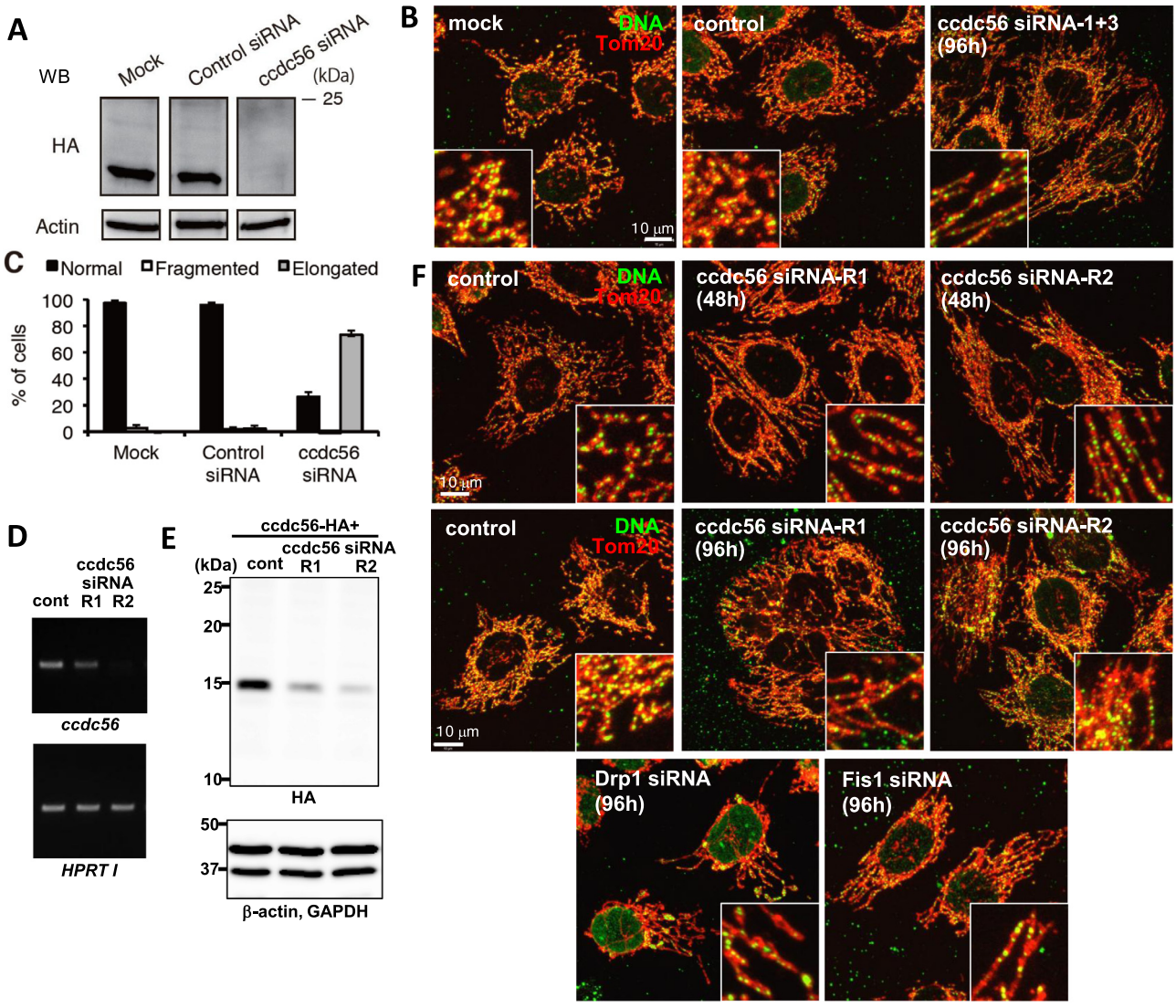

Fig. 2. Ccdc56 regulates mitochondrial morphology, but not mtDNA nucleoid structure, in HeLa cells. (A) HeLa cells transfected with a ccdc56-HA expression plasmid were treated with ccdc56-targeting siRNA duplexes (mixture of siRNA-1 and siRNA-3) or a control non-targeting siRNA duplex, or subjected to mock treatment, and then the production of ccdc56-HA was analyzed by immunoblotting using anti-HA antibodies. Different lanes from the same blot are shown. (B) HeLa cells were mock transfected or transfected with the control or ccdc56 siRNAs (1 + 3). After a 96-h incubation, the cells were subjected to indirect immunofluorescence analysis using the indicated antibodies. Tom20 is a mitochondrial protein (red). Anti-DNA specifically stained mtDNA (green). (C) The cells were stained and observed by confocal microscopy. Percentage of cells having normal, fragmented, elongated, or aggregated mitochondria. The data represent the mean ± S.D. of three independent experiments (100 cells scored per experiment). (D) HeLa cells were treated with ccdc56-targeting siRNA (siRNA-R1 or siRNA-R2) or a control siRNA for 96 h. The production of ccdc56 mRNA was analyzed by RT-PCR. (E) Repression of ccdc56 proteins was checked as in (A). (F) HeLa cells were transfected with the control or indicated siRNAs, cultured for 48 h or 96 h, and then subjected to indirect immunofluorescence analysis as in (B).

During investigation of the subcellular localization of ccdc56, we noticed that overproduction of ccdc56-HA resulted in aberrant mitochondrial morphology. As shown in Fig. 1E, HeLa cells overproducing ccdc56-HA ("high exp.") had fragmented mitochondria, instead of normal interconnected tubular mitochondria seen in cells moderately expressing ccdc56-HA ("low exp.").

Overexpression of ATAD3A also led to mitochondrial fragmentation similar to that observed for ccdc56 overexpression (Fig. 1E), as reported [8]. Quantitative analysis revealed that upon transient transfection with a ccdc56-HA expression plasmid, approximately 80% of HeLa cells producing ccdc56-HA contained fragmented mitochondria, whereas among the untransfected cells, such mitochondrial morphology was observed rarely (Fig. 1G). In contrast to the morphology of mitochondria, that of the ER was not affected by overproduction of ccdc56-HA, as observed on staining for the ER marker protein PDI (Fig. 1F), suggesting a specific effect of ccdc56-HA overproduction on mitochondrial morphology.

Next, we examined the effect of ccdc56 depletion by the introduction of ccdc56-targeting short-interfering RNA (siRNA) on mitochondrial morphology. To examine depletion efficiency, HeLa cells transfected with a ccdc56-HA expression plasmid were treated with ccdc56-specific siRNA or a control non-targeting siRNA, or subjected to mock treatment, and then the production of ccdc56-HA was analyzed by immunoblotting using anti-HA antibodies. As shown in Fig. 2A and E, treatment with the ccdc56-targeting siRNA, but not with the control siRNA or mock treatment, resulted in the almost complete inhibition of ccdc56-HA production, indicating the effectiveness of the ccdc56-targeting siRNA. When mitochondrial morphology was analyzed, the majority of ccdc56-depleted HeLa cells exhibited aberrant mitochondria with

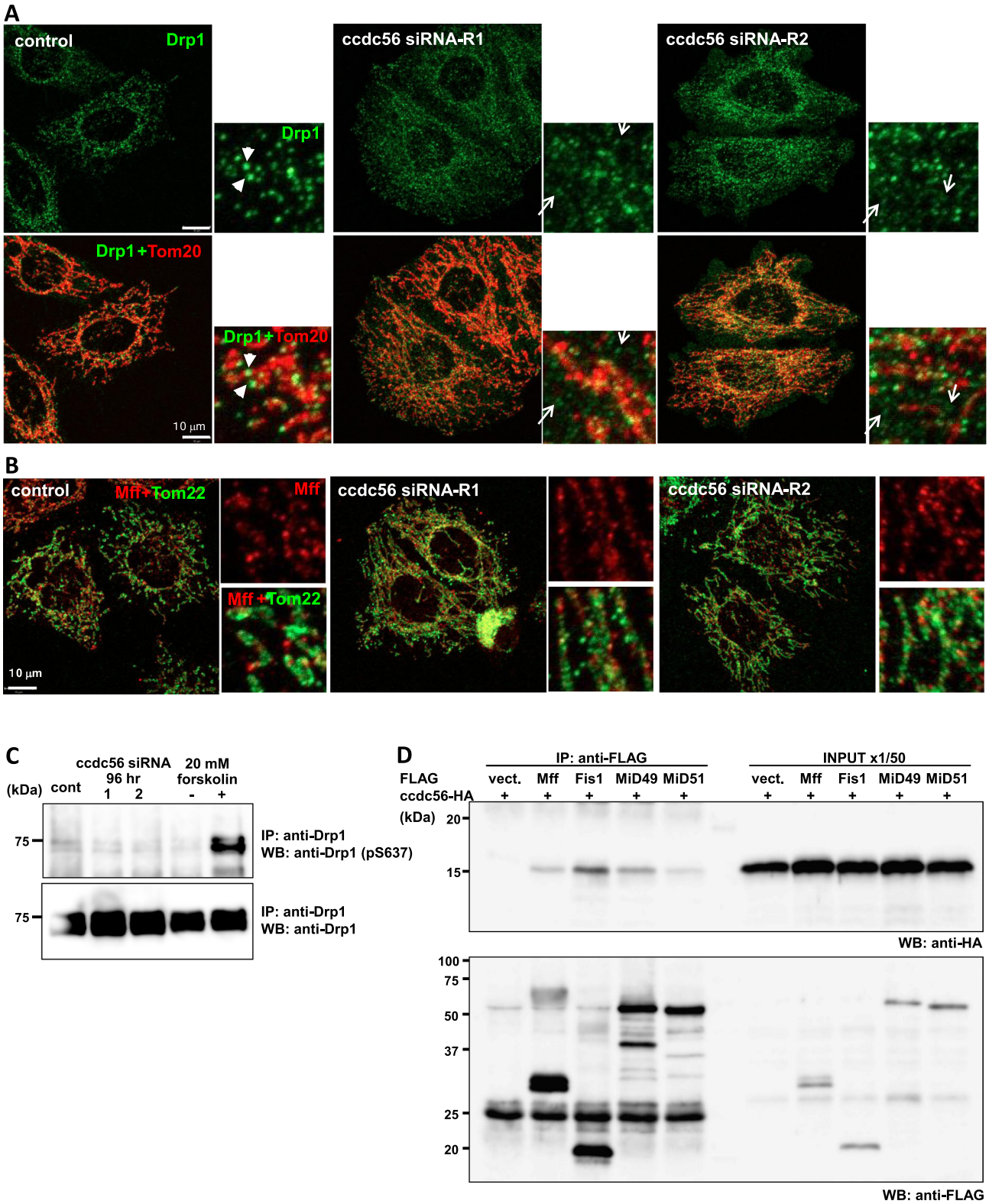

Fig. 3. Defective Drp1 targeting to mitochondria in ccdc56-deficient HeLa cells. (A and B) HeLa cells were treated with ccdc56-targeting siRNA (siRNA-R1 or siRNA-R2) or a control siRNA for 96 h. These cells were immunostained with the indicated antibodies. Tom20 and Tom22 were used as mitochondrial markers. Large Drp1 punctate structures were observed on the mitochondria of control cells (arrowheads), whereas smaller Drp1 puncta were observed in the cytoplasm (arrows) of ccdc56 siRNA-treated cells. (C) HeLa cells were transfected with ccdc56 or control siRNA, immunoprecipitated with an anti-Drp1 antibody, then analyzed by immunoblotting with the indicated antibodies. Forskolin was used as positive control. (D) HeLa cells were transfected with human ccdc56-HA with FLAG-tagged Mff, Fis1, MiD49, or MiD51. The cells were treated with 1% formaldehyde, immunoprecipitated with an anti-FLAG antibody, then analyzed by immunoblotting with anti-HA antibody.

elongated tubules, as seen in Drp1-repressed cells (Fig. 2B and F). Upon quantitative analysis, such aberrant mitochondria were observed in approximately 70% of the ccdc56-depleted cells, but were observed rarely in control siRNA-treated or mock-treated cells (Fig. 2C). This effect of ccdc56 depletion was suggested to be specific to mitochondrial morphology, because ccdc56-depleted

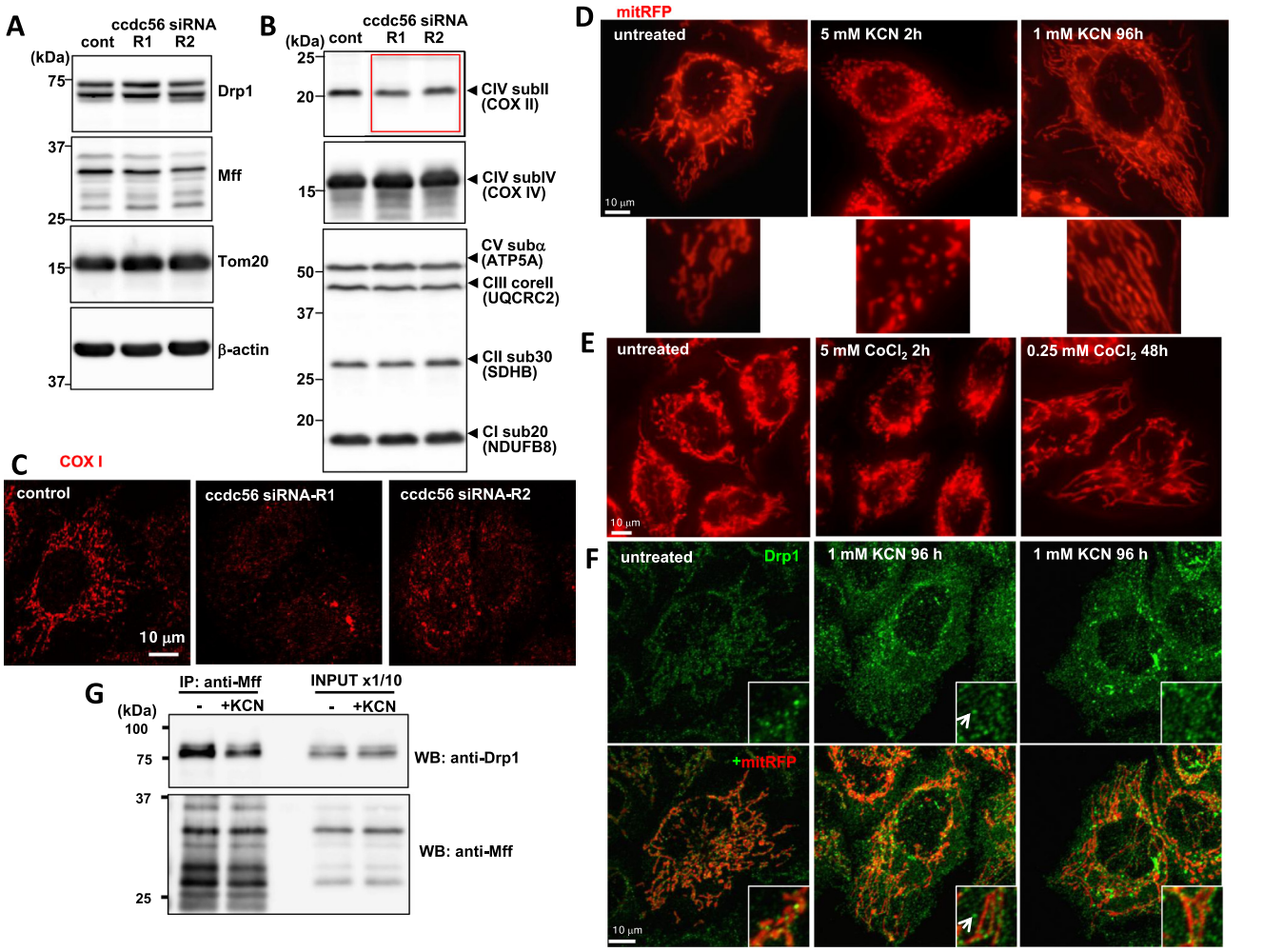

Fig. 4. COX assembly is partially defective in ccdc56-repressed cells, and mild COX inhibition leads to mitochondrial elongation. (A and B) HeLa cells treated with ccdc56-siRNA were analyzed by immunoblotting using the indicated antibodies. The expression of mitochondrial fission factors was normal (A), but the expression of the COX subunit COX II was partly diminished (indicated by the red rectangle). (C) Immunostaining using an anti-COX I antibody also supported the presence of partial defects in COX assembly. (D) HeLa cells were treated with 1 or 5 mM KCN for the indicated times, and mitochondrial morphology was analyzed by fluorescence microscopy. (E) HeLa cells were treated with 0.25 or 5 mM $CoCl_2$ for the indicated times, and mitochondrial morphology was analyzed by fluorescence microscopy. (F) HeLa cells expressing mitochondrial RFP were treated with 1 mM KCN for 96 h, and these cells were immunostained with anti-Drp1 antibodies. Drp1 puncta/aggregates were observed in the cytoplasm (arrows) in KCN-treated cells. (G) HeLa cells were treated with KCN as above, then these cells were treated with 1% formaldehyde, immunoprecipitated with an anti-Mff antibody, then analyzed by immunoblotting with the indicated antibodies.

HeLa cells exhibited normal ER morphology (data not shown). We further confirmed the repression of ccdc56 by RT-PCR (Fig. 2D), and which caused mitochondrial elongation (Fig. 2F) in HeLa cells treated with siRNAs to other target sequences of ccdc56.

Next, we analyzed the role of ccdc56 in mitochondrial morphogenesis. ATAD3 is a component of mtDNA nucleoids and plays a role in mtDNA maintenance [21]. However, the distribution of mtDNA nucleoids was not affected in ccdc56-repressed cells (Fig. 2B and C). It was reported that in ATAD3 repressed cells, mitochondrial morphology was less affected, or changed to small and fragmented mitochondria [17]. ATAD3 is known to be a multifunctional proteins [14–18,21], which might cause the different phenotype with that of ccdc56. Next, we analyzed the mitochondrial fission factor Drp1, which is a high-molecular-weight GTPase protein recruited from cytosol to mitochondrial fission sites that stimulates mitochondrial fission [5]. When we stained for Drp1 in control HeLa cells, many punctate structures were observed on the mitochondria (Fig. 3A, arrowheads). However, fewer Drp1 puncta were observed on the mitochondria of ccdc56-repressed cells, and instead, many small puncta were observed in cytosol (Fig. 3A, arrows). The expression level of Drp1 was normal in the ccdc56-repressed cells (Fig. 4A). Neither the expression (Fig. 4A) nor the distribution (Fig. 3B) of Mff, a mitochondrial receptor of Drp1, was affected. These data suggest that ccdc56 affects the mitochondrial targeting of Drp1. We then further analyzed molecular mechanism how mitochondrial morphology is regulated by ccdc56. Phosphorylation of Drp1 at Ser-637, which was modified under starvation condition [22], was not affected by ccdc56-repression (Fig. 3C), suggesting that the mitochondrial morphology change was not caused by energy exhaustion. Next we examined physical interaction of ccdc56 with mitochondrial fission factors by immunoprecipitation after cross-linking, and found that ccdc56 was co-precipitated with Drp1 receptors, Mff, MiD49, and MiD51, and a mitochondrial morphology protein Fis1 (Fig. 3D). Interestingly, ccdc56 was most efficiently recovered with Fis1 among these proteins, and Fis1-repressed cells, as well as ccdc56-repressed cells, exhibited aberrant mitochondria with elongated tubules (Fig. 2F). These data

suggested that ccdc56 is associated with the mitochondrial morphology factors, although it remains as an open question how inner membrane ccdc56 interacts with these outer membrane factors.

Recently, it was reported that ccdc56 mediates COX assembly [11–13]. COX II, analyzed by immunoblotting (Fig. 4B), and COX I, analyzed by immunofluorescence microscopy (Fig. 4C), were partly diminished in ccdc56-repressed cells, as shown previously [11–13]. It is well known that treatment with respiratory inhibitors, such as the protonophore CCCP or ATPase inhibitor oligomycin, leads to mitochondrial fragmentation by inhibiting Opa1-dependent mitochondrial fusion [23]. To elucidate the role of COX in mitochondrial morphology, we examined the effect of the COX inhibitor potassium cyanide (KCN) on mitochondrial morphology. When HeLa cells were treated with 5 mM KCN, the mitochondria fragmented immediately, as expected (Fig. 4D), and the cells died within several hours, possibly by severe COX inhibition. However, when COX activity was inhibited mildly by 1 mM KCN, the mitochondria were clearly and severely elongated after 4 days (Fig. 4D), suggesting that mild and chronic impairment of COX caused mitochondrial elongation, and which may correspond to the ccdc56-inhibition-induced mitochondrial elongation. We analyzed another COX-inhibiting condition by treating lower concentration of $CoCl_2$, which mimic hypoxia to block COX activity, and further confirmed that mild COX inhibition leads to mitochondrial elongation (Fig. 4E). In the KCN-treated cells, Drp1 was mislocalized in cytosol and formed punctate or aggregated structures (Fig. 4F). Furthermore, interaction between Drp1 and the mitochondrial receptor Mff was diminished (Fig. 4G). These data further support the conclusion that mild COX inhibition affects Drp1 localization and mitochondrial morphology.

Thus, we found that overproduction of ccdc56-HA induced fragmentation of mitochondria, and conversely, depletion of ccdc56 induced elongation of mitochondria and reduced the mitochondrial recruitment of Drp1. These data indicate that ccdc56 positively regulates mitochondrial fission. We further found that mild inhibition of the respiratory COX complex led to mitochondrial elongation. This is the first report to show a link between a COX assembly factor and mitochondrial fission. Ccdc56 interacts with the nucleoid protein ATAD3; however, ccdc56 had less of an impact on nucleoid distribution, suggesting that ATAD3 should have multiple functions, not only in mtDNA assembly but also affecting the COX assembly complex. It is an interesting question how the inner membrane protein ccdc56 regulates Drp1 targeting to the outer membrane, without affecting Mff. It might be possible that a partial COX defect induces a cellular stress response that affects mitochondrial morphology, as stress-induced mitochondrial hyperfusion [24]. However, the COX deficiency affected Drp1 recruitment, which is different from the mitochondrial hyperfusion regulated by Opa1 processing. Although the detailed molecular mechanism of how ccdc56 affects Drp1 targeting are unknown, further study of the function of ccdc56 will provide new insights into the mechanism and regulation of mitochondrial fission and biologically significant processes related to mitochondrial dynamic morphology, such as respiration, mammalian development, neurodegenerative diseases, and apoptosis.

Acknowledgements

We wish to thank Katsuyoshi Mihara and Toshihiko Oka for the antibodies, and Tadashi Ogishima, Sakae Kitada and Daniel Ken Inaoka for the discussions. This work was supported by Grant-in-Aid for Scientific Research from the Ministry of Education, Culture, Sports, Science and Technology of Japan (Grant Nos. 195900681 to O.K., 26291044 and 26111522 to N.I., 15K18534 to R.B.-I.).

References

[1] McBride, H.M., Neuspiel, M. and Wasiak, S. (2006) Mitochondria: more than just a powerhouse. Curr. Biol. 16, R551–R560.
[2] Cerveny, K.L., Tamura, Y., Zhang, Z., Jensen, R.E. and Sesaki, H. (2007) Regulation of mitochondrial fusion and division. Trends Cell Biol. 17, 563–569.
[3] Chan, D.C. (2006) Mitochondrial fusion and fission in mammals. Annu. Rev. Cell Dev. Biol. 22, 79–99.
[4] Hoppins, S., Lackner, L. and Nunnari, J. (2007) The machines that divide and fuse mitochondria. Annu. Rev. Biochem. 76, 751–780.
[5] Okamoto, K. and Shaw, J.M. (2005) Mitochondrial morphology and dynamics in yeast and multicellular eukaryotes. Annu. Rev. Genet. 39, 503–536.
[6] Detmer, S.A. and Chan, D.C. (2007) Functions and dysfunctions of mitochondrial dynamics. Nat. Rev. Mol. Cell Biol. 8, 870–879.
[7] Suen, D.F., Norris, K.L. and Youle, R.J. (2008) Mitochondrial dynamics and apoptosis. Genes Dev. 22, 1577–1590.
[8] Gilquin, B., Taillebourg, E., Cherradi, N., Hubstenberger, A., Gay, O., Merle, N., Assard, N., Fauvarque, M.O., Tomohiro, S., Kuge, O. and Baudier, J. (2010) The AAA+ ATPase ATAD3A controls mitochondrial dynamics at the interface of the inner and outer membranes. Mol. Cell. Biol. 30, 1984–1996.
[9] Ban-Ishihara, R., Ishihara, T., Sasaki, N., Mihara, K. and Ishihara, N. (2013) Dynamics of nucleoid structure regulated by mitochondrial fission contributes to cristae reformation and release of cytochrome c. Proc. Natl. Acad. Sci. U.S.A. 110, 11863–11868.
[10] Ban, R., Matsuzaki, H., Akashi, T., Sakashita, G., Taniguchi, H., Park, S.Y., Tanaka, H., Furukawa, K. and Urano, T. (2009) Mitotic regulation of the stability of microtubule plus-end tracking protein EB3 by ubiquitin ligase SIAH-1 and aurora mitotic kinases. J. Biol. Chem. 284, 28367–28381.
[11] Peralta, S., Clemente, P., Sanchez-Martinez, A., Calleja, M., Hernandez-Sierra, R., Matsushima, Y., Adan, C., Ugalde, C., Fernandez-Moreno, M.A., Kaguni, L.S. and Garesse, R. (2012) Coiled Coil Domain-containing Protein 56 (CCDC56) is a novel mitochondrial protein essential for cytochrome c oxidase function. J. Biol. Chem. 287, 24174–24185.
[12] Clemente, P., Peralta, S., Cruz-Bermudez, A., Echevarria, L., Fontanesi, F., Barrientos, A., Fernandez-Moreno, M.A. and Garesse, R. (2013) HCOA3 stabilizes cytochrome c oxidase 1 (COX1) and promotes cytochrome c oxidase assembly in human mitochondria. J. Biol. Chem. 288, 8321–8331.
[13] Mick, D.U., Dennerlein, S., Wiese, H., Reinhold, R., Pacheu-Grau, D., Lorenzi, I., Sasarman, F., Weraarpachai, W., Shoubridge, E.A., Warscheid, B. and Rehling, P. (2012) MITRAC links mitochondrial protein translocation to respiratory-chain assembly and translational regulation. Cell 151, 1528–1541.
[14] Geuijen, C.A. et al. (2005) A proteomic approach to tumour target identification using phage display, affinity purification and mass spectrometry. Eur. J. Cancer 41, 178–187.
[15] Schaffrik, M., Mack, B., Matthias, C., Rauch, J. and Gires, O. (2006) Molecular characterization of the tumor-associated antigen AAA-TOB3. Cell. Mol. Life Sci. 63, 2162–2174.
[16] Bogenhagen, D.F., Rousseau, D. and Burke, S. (2008) The layered structure of human mitochondrial DNA nucleoids. J. Biol. Chem. 283, 3665–3675.
[17] He, J. et al. (2007) The AAA+ protein ATAD3 has displacement loop binding properties and is involved in mitochondrial nucleoid organization. J. Cell Biol. 176, 141–146.
[18] Wang, Y. and Bogenhagen, D.F. (2006) Human mitochondrial DNA nucleoids are linked to protein folding machinery and metabolic enzymes at the mitochondrial inner membrane. J. Biol. Chem. 281, 25791–25802.
[19] Gerhard, D.S. et al. (2004) The status, quality, and expansion of the NIH full-length cDNA project: the Mammalian Gene Collection (MGC). Genome Res. 14, 2121–2127.
[20] Strausberg, R.L. et al. (2002) Generation and initial analysis of more than 15,000 full-length human and mouse cDNA sequences. Proc. Natl. Acad. Sci. U.S.A. 99, 16899–16903.
[21] He, J., Cooper, H.M., Reyes, A., Di Re, M., Sembongi, H., Litwin, T.R., Gao, J., Neuman, K.C., Fearnley, I.M., Spinazzola, A., Walker, J.E. and Holt, I.J. (2012) Mitochondrial nucleoid interacting proteins support mitochondrial protein synthesis. Nucleic Acids Res. 40, 6109–6121.
[22] Gomes, L.C., Di Benedetto, G. and Scorrano, L. (2011) During autophagy mitochondria elongate, are spared from degradation and sustain cell viability. Nat. Cell Biol. 13, 589–598.
[23] Sekine, S., Kanamaru, Y., Koike, M., Nishihara, A., Okada, M., Kinoshita, H., Kamiyama, M., Maruyama, J., Uchiyama, Y., Ishihara, N., Takeda, K. and Ichijo, H. (2012) Rhomboid protease PARL mediates the mitochondrial membrane potential loss-induced cleavage of PGAM5. J. Biol. Chem. 287, 34635–34645.
[24] Tondera, D., Grandemange, S., Jourdain, A., Karbowski, M., Mattenberger, Y., Herzig, S., Da Cruz, S., Clerc, P., Raschke, I., Merkwirth, C., Ehses, S., Krause, F., Chan, D.C., Alexander, C., Bauer, C., Youle, R., Langer, T. and Martinou, J.C. (2009) SLP-2 is required for stress-induced mitochondrial hyperfusion. EMBO J. 28, 1589–1600.